Catal Lett (2009) 129:194–206
DOI 10.1007/s10562-008-9790-0

# Preparation of Highly Dispersive and Stable Platinum Catalysts Supported on Siliceous SBA-15 Mesoporous Material: Roles of Titania Layer Incorporation and Hydrogen Peroxide Treatment

**Mi-Young Kim · Se Bi Jung · Min Gyu Kim · Young San You · Jung-Hyun Park · Chae-Ho Shin · Gon Seo**

Received: 2 October 2008 / Accepted: 17 November 2008 / Published online: 4 December 2008


**Abstract** Roles of titania layer incorporation and hydrogen peroxide treatment in the preparation of highly dispersed platinum catalysts supported on siliceous SBA-15 mesoporous materials were studied by examining the catalysts at each step of the preparation. XRD, TEM, XPS, Raman, IR, CO chemisorptions, EXAFS and XANES techniques were employed to the investigation of the physico-chemical states of platinum and titanium. The platinum particles were uniformly dispersed on SBA-15 ranged from 1 to 2 nm in size by incorporating titania onto the surface of SBA-15 and then treating the impregnating platinum precursor with hydrogen peroxide, even at platinum loading as high as 4 wt.%. The platinum catalysts showed considerably higher catalytic activity in the combustion reactions of both carbon monoxide and methane, suggesting a suitable catalyst for purifying diesel engine exhaust.

**Electronic supplementary material** The online version of this article (doi:10.1007/s10562-008-9790-0) contains supplementary material, which is available to authorized users.

M.-Y. Kim · S. B. Jung · G. Seo (✉)
School of Applied Chemical Engineering and Center for Functional Nano Fine Chemicals, Chonnam National University, Youngbong-Dong 300, Gwangju 500-757, Republic of Korea
e-mail: gseo@chonnam.ac.kr

M. G. Kim
Pohang Accelerator Laboratory, San-31 Hyoja-Dong, Pohang, Kyungbuk 790-784, Republic of Korea

Y. S. You
Heesung Catalysts Corp., 1251-6 Jungwang-Dong, Shihung, Geonggi 429-450, Republic of Korea

J.-H. Park · C.-H. Shin
Department of Chemical Engineering, Chungbuk National University, Cheongju, Chungbuk 361-763, Republic of Korea

**Keywords** Platinum · Dispersion · Silica · Titania incorporation · Hydrogen peroxide treatment

## 1 Introduction

Platinum catalysts have been widely used in hydrogenation and dehydrogenation processes of the petrochemical industry, and have recently become more important as purifying catalysts of automobile exhaust pollutants and as combustion catalysts for volatile organic compounds [1]. Furthermore, the amount of platinum consumed increases rapidly in the active phase of electrode catalysts of fuel cells [2].

Since platinum is neither mechanically strong nor stable at high temperature, highly stable porous supports are usually employed to prepare highly dispersive and stable platinum catalysts [3]. Reducing the loading amount of platinum catalysts by increasing the dispersion lowers the production cost of platinum catalysts with high catalytic activity. Alumina, titania and ceria with high surface area and high mechanical stability are generally used as supports [4–6]. Carbon and silica supports make it possible to prepare non-acidic platinum catalysts suitable for organic reactions by enhancing the interaction between reactants and catalysts without accelerating the acid-catalyzed side reactions [7, 8]. Among these catalyst supports, silica features the good properties of chemical inertness, high thermal stability and good processibility. However, the weak interaction between platinum and silica induces severe *sintering* of platinum in a reductive atmosphere, resulting in the rapid deactivation of the platinum catalysts supported on the silica [9]. $\gamma$-alumina has been considered to be suitable for preparing highly dispersed platinum catalysts due to its weak acidity which enhances the

interaction between platinum and alumina, even though alumina accelerates acid-catalyzed side reactions, thereby lowering the selectivity for desired products [10].

A study on the preparation of platinum catalysts on alumina suggested that both platinum precursors and calcination procedures are important to achieve high platinum dispersion [11]. The pretreatment in different gas environments was also crucial for the dispersion of platinum supported on silica [12]. The autoreduction of platinum catalysts at low temperature produced small platinum particles by avoiding the formation of large *sinterings*. The careful temperature-programmed decomposition of platinum tetraamine hydroxide impregnated on silica was recommended to obtain high platinum dispersion at loadings up to 5 wt.% [13]. However, platinum catalysts supported on silica usually show a rapid decrease in the platinum dispersion at higher temperatures. At temperatures above 500 °C, the dispersion usually falls to 20% in even an oxidation atmosphere because of the weak interaction between platinum and silica.

We previously reported a preparation method for highly dispersive and stable platinum catalysts supported on silica by incorporating titania layer onto it and treating the impregnated platinum precursor with hydrogen peroxide [14]. The interaction between platinum and the titania layer incorporated onto the silica support provides high stability and high platinum dispersion. The platinum particles range 1–2 nm in size, even at a platinum loading as high as 4 wt.%. The platinum catalysts supported on titania-incorporated silica show different behavior from those supported on alumina due to the strong metal support interaction (SMSI). The suppression of hydrogen adsorption on platinum due to its interaction with titania results in the poor hydrogenation activity of the platinum catalysts in the hydrogenation of nitrobenzene [15]. On the contrary, their activity in the oxidation of carbon monoxide remains high despite the limited adsorption of carbon monoxide on the catalysts. Nevertheless, the roles of the titania layer incorporated onto silica and of the treatment of the platinum precursor incorporated with hydrogen peroxide in their preparation steps have not been well elucidated.

Therefore, we examined the physico-chemical states of platinum and titanium at each step of the preparation of platinum catalysts supported on SBA-15 mesoporous material using XRD, TEM, XPS, Raman, IR, CO chemisorptions, EXAFS and XANES techniques in order to examine the contributions of the titania layer incorporated onto silica and the hydrogen peroxide treatment on the dispersion and stability of the platinum supported on silica. Because amorphous silica has no long-range order of the positions of the atoms, a SBA-15 mesoporous material made of silica only, is suitable to obtain definite spectroscopic observation. The SBA-15 mesoporous silica material has large surface areas and well-defined surface properties for incorporating titania on the silica surface. It also has thick pore wall (2–6 nm), resulting in improving hydrothermal stability. Furthermore, its uniform pores provide good accessibility for reactants [16, 17]. In this study, we used an anionic form precursor of platinum to intensify the effects of the titania incorporation and the hydrogen peroxide treatment on the dispersion and stability of platinum, even though its anionic precursors usually result in poor platinum dispersion due to the negative $\zeta$-potential of the silica surface [18]. The adsorption of benzaldehyde on the platinum catalysts was also studied using in situ FT-IR spectroscopy to observe the change in the titania with the reduction in its dispersion and chemical states [19, 20]. The activity of the platinum catalysts in the combustion reactions of methane and carbon monoxide was also discussed relating to their application as diesel oxidation catalysts.

## 2 Experimental

### 2.1 Preparation of Catalysts

A SBA-15 mesoporous material was prepared using poly(ethylene glycol)-*block*-poly(propylene glycol)-*block*-poly(ethylene glycol) copolymer (P-123, $M_{avg} = 5{,}800$, Aldrich) as a template following the procedure described in the literature [21]. The template was dissolved in deionized water at 40 °C with stirring. Hydrogen chloride solution and tetraethylorthosilicate (98%, Aldrich) added to the P-123 solution which was then stirred for 20 h. The synthetic mixture was hydrothermally reacted at 100 °C for 20 h. The solid phase obtained from the synthetic mixture was filtered and washed with deionized water. The obtained SBA-15 was dried to a solid phase at 100 °C and then calcined at 550 °C for 8 h to remove the template.

After removing the water contained in the SBA-15 by extracting with anhydrous ethanol (99.9%, Duksan), titania butoxide (>99%, Johnson Matthey Co.) dissolved in anhydrous ethanol was added to the SBA-15 slurry to incorporate a titania layer on the SBA-15 followed the procedure described in our previous paper [14]. An anionic platinum precursor, hydrogen hexahydroxyplatinate (99.9%, Aldrich), was impregnated on the titania-incorporated SBA-15 by an incipient wetness method. After drying the SBA-15 impregnated with the platinum precursor at 80 °C for 12 h, it was treated with hydrogen peroxide (30%, Daejung) at 60 °C for 1 h. The platinum catalyst supported on the titania-incorporated SBA-15 and prepared by treating with hydrogen peroxide was obtained by reducing the calcined catalysts in a reductive flow ($H_2/N_2 = 50/50$ as vol.%) of 100 mL $min^{-1}$ at 400 °C for

2 h. The platinum catalyst prepared was named $H_2O_2$–Pt/$TiO_2$–SBA-15 in accordance with its preparation procedure.

For comparison, the following three platinum catalysts were prepared: direct on the SBA-15 (Pt/SBA), on the titania-incorporated SBA-15 (Pt/$TiO_2$–SBA), and on the titania-incorporated SBA-15 which had been treated with hydrogen peroxide prior to the impregnation of the platinum precursor (Pt/$H_2O_2$–$TiO_2$–SBA). The amount of platinum impregnated on the platinum catalysts was set high to 4 wt.% to observe the difference in the platinum dispersion according to their preparation methods.

### 2.2 Characterization of the Prepared Platinum Catalysts

The titania and platinum contents of the prepared platinum catalysts were determined using an EDX system equipped on a SEM (S-4700/Horia, EX-200, Hitachi).

The spectroscopic methods such as XRD, TEM and XPS for the characterization of the platinum catalysts were described in our previous paper [14]. The procedure for the measurement of nitrogen adsorption isotherm of the SBA-15 was also described in the same paper. Raman spectroscopy was performed using a SPEX 1403 spectrometer using a laser of 514 nm wavelength.

X-ray absorption spectra (XANES and EXAFS) of the titanium and platinum atoms of the platinum catalysts were recorded at the 7C1 beamline of the Pohang Accelerator Laboratory. X-ray spectra were monochromated by a double crystal monochromator composed of Si(111) and Si(311) crystals. The measurement of X-ray absorption by the samples was carried out in a helium flow to minimize their changes in chemical states. The X-ray absorption of titanium atoms was measured in a transmission mode around the Ti K-edge (4,966 eV) by detuning in the range of 70–80% to eliminate higher harmonics. The X-ray absorption of platinum atoms was measured around the Pt $L_{III}$-edge (11,564 eV). Radial distributions of titania and platinum were obtained from the Fourier-transformed absorption data and analyzed using XFIT software based on the FEFF8.1 theoretical model.

EXAFS spectra of platinum dispersed on the platinum catalysts were also recorded in situ using a *Lab*-EXAFS spectrometer (R-XAS, Rikagu, Japan). A specially designed in situ cell was installed between an Ar detector ($I_0$) and a scintillation detector ($I$) for the measurement of X-ray absorption in a transmission mode [22]. The samples mounted in the in situ cell were evacuated at 200 °C for 2 h and cooled to 25 °C. The reduction of the samples were carried out at a reductive flow ($H_2$/He = 10/90 as vol.%) at 200 and 400 °C. After reduction for 2 h, EXAFS spectra of platinum at the Pt $L_{III}$-edge were recorded.

The amounts of carbon monoxide adsorbed on the platinum catalysts were measured using a chemisorption apparatus (BEL-CAT, BEL, Japan). The catalyst samples activated in a helium flow at 400 °C for 2 h were cooled to 50 °C and then saturated with pulses of carbon monoxide (CO/He = 5/95 as vol.%). The amount of carbon monoxide adsorbed was calculated from the amount removed due to chemisorption.

The IR spectra of benzaldehyde adsorbed on the $H_2O_2$–Pt/$TiO_2$–SBA catalyst were recorded on an FT-IR spectrophotometer (Bio-Rad, FTS 175C). A self-supported catalyst wafer of 5 mg was evacuated at 400 °C for 1 h (as calcined) and reduced by exposing to hydrogen of 30 Torr repeatedly at the same temperature (as reduced). IR spectra of benzaldehyde adsorbed on it were recorded at 100 °C after flowing benzaldehyde (Aldrich, 99%) vapor diluted in a helium flow of 50 mL $min^{-1}$. Benzaldehyde weakly adsorbed was removed before recording by purging with the helium flow for 30 min. $TiO_2$–SBA was employed as a reference material in the adsorption of benzaldehyde.

### 2.3 Catalytic Reactions over the Platinum Catalysts

The catalytic combustion of methane was carried out in a continuous-flow, fixed-bed reaction system with a quartz reactor (I.D. = 12 mm) operated at atmospheric pressure. The platinum catalyst (0.1 g) was diluted with 1 g of SiC (Aldrich) powder to minimize the change in reaction temperature due to the heat of combustion. A K-type thermocouple was placed at the center of the catalyst bed. Prior to the catalytic run, the charged platinum catalyst was pretreated under a helium flow of 200 $cm^3$ $min^{-1}$ at 600 °C for 1 h, and then cooled to the desired reaction temperature. The reactant gas composed of 1.0% $CH_4$ and 4% $O_2$ in He balance was fed into the quartz reactor. The total gas flow at the reactor inlet was maintained at 200 $cm^3$ $min^{-1}$. The performance of the platinum catalysts in the methane combustion was continuously measured by increasing the reaction temperature from 200 to 600 °C at a heating the rate of 2 °C $min^{-1}$.

For the oxidation of carbon monoxide, a mixture of 0.05 g of platinum catalyst and 1 g of SiC was charged in the reactor. The charged catalyst was activated in the helium flow at 400 °C for 1 h prior to the catalytic reaction. The reaction gas composed of 1.0% CO and 4% $O_2$ in He balance was fed at a total flow rate of 200 $cm^3$ $min^{-1}$ at atmospheric pressure. The performance of the platinum catalysts in the oxidation of carbon monoxide was continuously measured by increasing the reaction temperature from 100 to 300 °C at a heating rate of 2 °C $min^{-1}$.

The conversions of methane and carbon monoxide in their combustion reactions were calculated in terms of their percentages consumed. Their concentrations in the product

stream were analyzed every 5 s by using an on-line $CH_4$/CO IR analyzer (TELEDYNE Analytical Instruments 7500 Model).

## 3 Results and Discussion

The XRD pattern and nitrogen adsorption isotherm of the prepared SBA-15 are shown in Fig. S1 (see supplement). The strong peak observed in the diffraction pattern at $2\theta = 0.85°$ indicated the presence of uniform mesopores. The nitrogen adsorption isotherm also exhibited a distinct hysteresis at $P/P_0 = 0.65$–$0.8$ due to its mesopores. The average diameter of the mesopores determined by the Barrett–Joiner–Halenda method was 5.4 nm, its surface area calculated by the Brunauer–Emmett–Teller equation was 850 $m^2\ g^{-1}$, and its pore volume was 1.3 $cm^3\ g^{-1}$.

Figure 1 shows the XRD patterns of the platinum catalysts supported on the SBA-15. A broad peak around $2\theta = 22°$ was attributed to silica. No diffraction peak relative to crystalline titania was evident on Pt/$TiO_2$–SBA and $H_2O_2$–Pt/$TiO_2$–SBA, despite the high titania contents (up to 10%) incorporated onto them, as listed in Table 1. Only a small peak attributed to anatase appeared at around $2\theta = 25°$ on Pt/$H_2O_2$–$TiO_2$–SBA.

The diffraction peaks attributed to the platinum of the platinum catalysts considerably differed according to their preparation methods. The Pt/SBA and Pt/$H_2O_2$–$TiO_2$–SBA catalysts showed intense diffraction peaks of platinum metal at $2\theta = 39.6$, 46.2 and 67.4°. The appearance of distinct diffraction peaks relative to a metallic platinum phase indicated the *sintering* of platinum on these catalysts. The diffraction peaks of platinum were small on Pt/$TiO_2$–SBA, but $H_2O_2$–Pt/$TiO_2$–SBA did not show any diffraction peaks relative to platinum metal. These results indicated the significant improvement of platinum dispersion on the Pt/$TiO_2$–SBA and $H_2O_2$–Pt/$TiO_2$–SBA catalysts compared to those on the Pt/SBA and Pt/$H_2O_2$–$TiO_2$–SBA catalysts. The average platinum particle size on Pt/SBA calculated using the Scherrer equation from its diffraction peaks was large at around 20 nm, but it was impossible to determine the size of the platinum particles on $H_2O_2$–Pt/$TiO_2$–SBA from its diffraction pattern. The incorporation of a titania layer on the SBA-15 considerably improved the platinum dispersion, which was additionally enhanced by the further treatment of the impregnated platinum precursor with hydrogen peroxide. On the contrary, the treatment of the titania-incorporated SBA with hydrogen peroxide prior to the impregnation of the platinum precursor did not improve the platinum dispersion, as shown on the XRD pattern of Pt/$H_2O_2$–$TiO_2$–SBA.

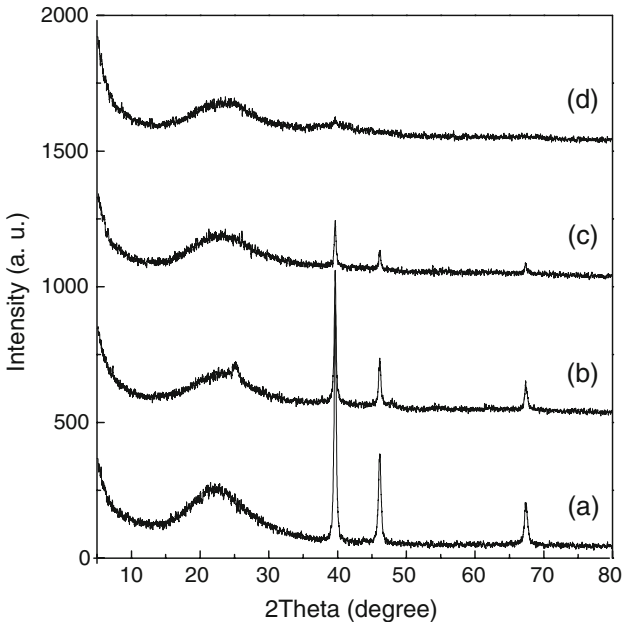


**Fig. 1** X-ray diffraction patterns of **a** Pt/SBA, **b** Pt/$H_2O_2$–$TiO_2$–SBA, **c** Pt/$TiO_2$–SBA and **d** $H_2O_2$–Pt/$TiO_2$–SBA catalysts

The XRD patterns of the Pt/SBA and $H_2O_2$–Pt/$TiO_2$–SBA catalysts recorded as a function of temperature in the reductive atmosphere, shown in Fig. 2, clearly presented their variation in the stability of the platinum particles against sintering. Pt/SBA showed sharp diffraction peaks relative to metallic platinum, even after reduction at 400 °C. The peaks considerably increased following treatment in the reductive flow at 550 °C. On the contrary, there were no diffraction peaks relative to metallic platinum on $H_2O_2$–Pt/$TiO_2$–SBA at its reduced state. Small diffraction peaks of metallic platinum appeared after treatment at 550 °C, and no further increase in its diffraction peaks was observed even after treatment at 850 °C.

This clear difference in the diffraction patterns of Pt/SBA and $H_2O_2$–Pt/$TiO_2$–SBA according to their preparation methods demonstrated the significant enhancement of the dispersion and stability of platinum gained by the titania incorporation and the subsequent hydrogen peroxide treatment. The platinum supported on the SBA-15 rapidly sintered to large particles in the reductive atmosphere. However, the maintenance of very small diffraction peaks relative to the metallic platinum of $H_2O_2$–Pt/$TiO_2$–SBA, even after the reduction at 850 °C, indicated the exceptional dispersion and stability of the platinum particles.

Figure 3 shows TEM images of the platinum catalysts. Large particles with diameters of 20–50 nm were observed on Pt/SBA. The platinum particles dispersed on Pt/$H_2O_2$–$TiO_2$–SBA were very small, but large particles of platinum were observed together. The hydrogen peroxide treatment on platinum precursor impregnated on titania layer enhanced more uniform dispersion of platinum by increasing the reaction feasibility between platinum

**Table 1** Composition and platinum dispersion of catalysts prepared

| Catalyst | Composition[a] (wt.%) | | CO adsorption[b] ($cm^3\ g^{-1}$) | Pt dispersion[c] (%) | $T_{50\%}$[d] (°C) | |
|---|---|---|---|---|---|---|
| | Pt | Ti | | | CO | $CH_4$ |
| Pt/SBA | 3.9 | – | 0.035 | – | – | – |
| Pt/$H_2O_2$–$TiO_2$–SBA | 3.8 | 9.9 | 0.064 | – | 209 | 593 |
| Pt/$TiO_2$–SBA | 3.4 | 10.2 | 0.286 | 24 | 193 | 589 |
| $H_2O_2$–Pt/$TiO_2$–SBA | 3.7 | 10.3 | 0.134 | 87 | 188 | 484 |

[a] Measured by EDX

[b] Measured by chemisorption at 50 °C

[c] Calculated from TEM photos

[d] Defined as the temperature at which the conversion of a reactant reaches to 50%

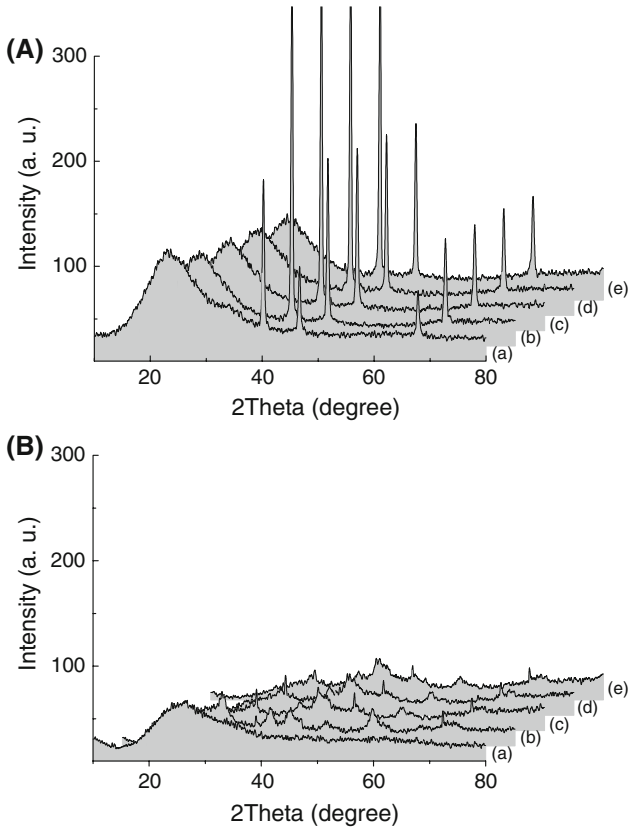


**Fig. 2** X-ray diffraction patterns of **A** Pt/SBA and **B** $H_2O_2$–Pt/$TiO_2$–SBA catalysts obtained at elevated temperatures in reductive atmosphere at (a) 25, (b) 550, (c) 650, (d) 750 and (e) 850 °C. The catalysts were evacuated at 500 °C for 1 h before exposing to hydrogen

precursor and peroxo ion formed on the titania layer. Pt/$TiO_2$–SBA prepared by impregnating the platinum precursor on the titania-incorporated SBA-15 showed uniformly dispersed platinum particles of 3–7 nm. Platinum particles of 1–2 nm in diameter were uniformly dispersed on $H_2O_2$–Pt/$TiO_2$–SBA, presenting an exceptionally good dispersion. As mentioned above (Fig. 1), the titania incorporation was effective to enhance the platinum dispersion on the SBA-15, and the additional hydrogen peroxide treatment of the impregnated platinum precursor afforded exceptionally high platinum dispersion on $H_2O_2$–Pt/$TiO_2$–SBA. Even at a platinum loading on the platinum catalyst as high as 4 wt.%, high platinum dispersion was achieved on the siliceous support SBA-15.

The dark field image of $H_2O_2$–Pt/$TiO_2$–SBA shown in Fig. 4 clearly indicated the strong interaction between platinum and titania. The titania layer in dark field image appeared brighter than the silica opposite to it in the bright field image. The EDX spectrum of the bright part was composed of platinum and titanium, whereas the predominant element of the dark part was silicon. These clear differences in distribution among silicon, titanium and platinum were due to the interaction between platinum and titania. The exceptionally high platinum dispersion on the titania-incorporated SBA-15 was primarily responsible for the titania layer incorporated onto it, inducing the SMSI with platinum and maintaining the high dispersion of platinum even at high temperature [23–25].

The XPS spectra of the platinum catalysts supported on the SBA-15 revealed further information about the changes in the physical property and chemical state of platinum and titanium during their preparation. Figure 5 shows the XPS spectra of the platinum catalysts recorded at their dried state after impregnating the platinum precursor and at their reduced state. The Pt 4f peaks were composed of paired peaks of Pt $4f_{5/2}$ and Pt $4f_{7/2}$, in which the binding energies of the large Pt $4f_{7/2}$ peaks at platinum metal, platinum species of 2+, and platinum species of 4+ were observed at 71.5, 72.7, and 74.0 eV, respectively [6]. The Pt $4f_{7/2}$ peaks observed on Pt/SBA after drying had binding energies of 72.4 and 74.2 eV, indicating the presence of $Pt^{2+}$ and $Pt^{4+}$ together (see supplement Table S1). Some of the platinum was reduced from $Pt^{4+}$ of hydrogen hexahydroxyplatinate to $Pt^{2+}$ by only drying the impregnated platinum precursor [15]. The platinum impregnated on Pt/$TiO_2$–SBA, Pt/$H_2O_2$–$TiO_2$–SBA and $H_2O_2$–Pt/$TiO_2$–SBA also had twin oxidized states of +2 and +4, as in the case of Pt/SBA.

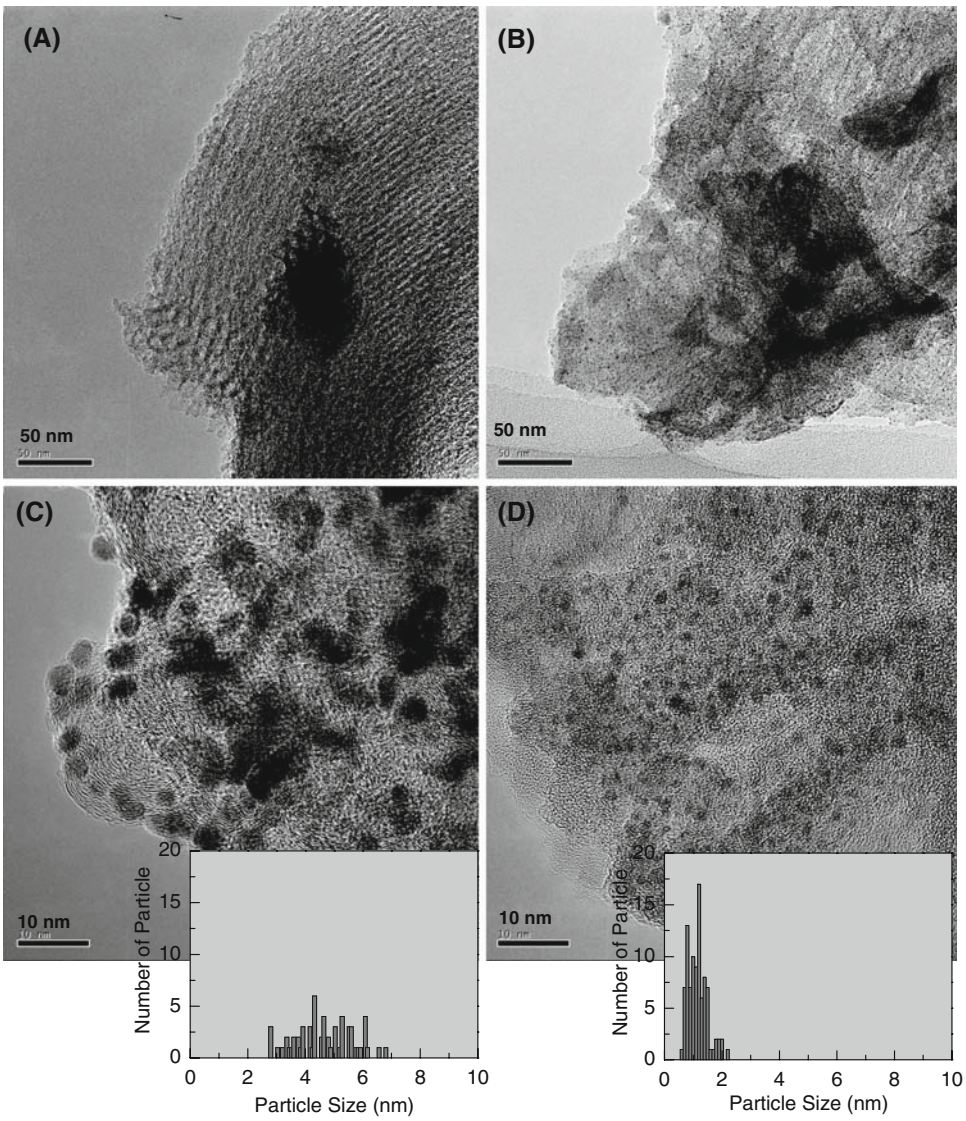


**Fig. 3** TEM images of **a** Pt/SBA, **b** $Pt/H_2O_2$–$TiO_2$–SBA, **c** $Pt/TiO_2$–SBA and **d** $H_2O_2$–$Pt/TiO_2$–SBA catalysts

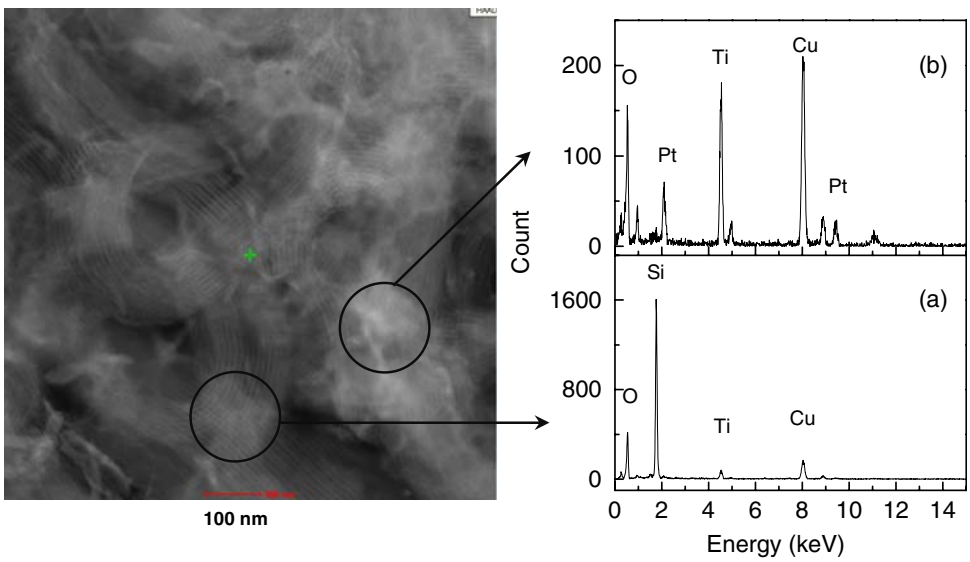


**Fig. 4** Dark field image and EDX spectra of $H_2O_2$–$Pt/TiO_2$–SBA catalyst: **a** SBA-15 support itself and **b** platinum on titania

The peak areas of platinum $4f_{5/2}$ and $4f_{7/2}$ strongly depended on the preparation method of the platinum catalysts. Pt/SBA had the smallest peak area, and $H_2O_2$–Pt/$TiO_2$–SBA the largest. Even in the dried states, the platinum dispersion on the platinum catalysts increased in the order of Pt/SBA < Pt/$H_2O_2$–$TiO_2$–SBA ≈ Pt/$TiO_2$–SBA < $H_2O_2$–Pt/$TiO_2$–SBA. The interaction between platinum and titania enhanced the platinum dispersion.

The chemical state of platinum in the platinum catalysts at their reduced states also differed according to their preparation methods. The large peak area of platinum on $H_2O_2$–Pt/$TiO_2$–SBA indicated its high platinum dispersion. The binding energy of the metallic Pt $4f_{7/2}$ peak of the platinum catalysts varied: 71.8 eV for Pt/SBA, 71.5 eV for Pt/$TiO_2$–SBA, and 71.1–71.2 eV for Pt/$H_2O_2$–$TiO_2$–SBA and $H_2O_2$–Pt/$TiO_2$–SBA. The platinum dispersed on Pt/SBA had the typical binding energy of platinum metal, while that on the titania-incorporated SBA-15 presented a small shift of the binding energy from 71.8 to 71.1 eV. Since a smaller binding energy of platinum corresponds to its high electron density [15], the titania layer incorporated onto the SBA-15 increased the electron density of platinum dispersed on it.

In addition, the platinum catalysts supported on the titania-incorporated SBA-15, Pt/$TiO_2$–SBA, Pt/$H_2O_2$–$TiO_2$–SBA and $H_2O_2$–Pt/$TiO_2$–SBA all showed small platinum Pt $4f_{7/2}$ peaks relative to the oxidized state of +2. These peaks strongly suggested that some of the platinum retained its oxidized state even after being reduced at 400 °C. Following their dispersal on the titania layer, some of the platinum atoms had oxygen atoms as the nearest neighbor.

The XPS spectra of the Ti $2p_{3/2}$ and O 1s peaks of the platinum catalysts supported on the titania-incorporated SBA-15 are shown in Fig. 6. The Ti $2p_{3/2}$ peaks observed from the platinum catalysts had a maximum around 459 eV. The titania with tetrahedral coordination shows its Ti $2p_{3/2}$ peak at 458.4 eV [26]. The negligible difference of their Ti $2p_{3/2}$ peaks between the dried and reduced states suggested that the titanium atoms incorporated onto the SBA-15 had a tetrahedral coordination even at the incorporation step, regardless of the preparation method. XANES spectra of Ti K-edge shown in Fig. S2 (see supplement) strongly indicated the tetrahedral coordination of titania atoms [27]. However, the binding energy of the Ti $2p_{3/2}$ peaks of the platinum catalysts exhibited a slight difference due to the hydrogen peroxide treatment. The peak maximum of the Ti $2p_{3/2}$ peak on Pt/$TiO_2$–SBA was 459.2 eV, compared to 458.7 eV for both Pt/$H_2O_2$–$TiO_2$–SBA and $H_2O_2$–Pt/$TiO_2$–SBA. The small lowering shift of the Ti $2p_{3/2}$ peak of the platinum catalysts by the hydrogen peroxide treatment indicated that the treatment caused to enhance the content of titanium atoms with definite tetrahedral coordination [26].

The hydrogen peroxide treatment of the platinum catalysts and the reduction in the reductive flow affected the O 1s peaks of Pt/$TiO_2$–SBA, and its peak maximum was therefore observed at 532.9 eV. However, the O 1s peaks of Pt/$H_2O_2$–$TiO_2$–SBA and $H_2O_2$–Pt/$TiO_2$–SBA differed in terms of their binding energy and shape. The O 1s peaks on these hydrogen peroxide-treated platinum catalysts were composed of a large peak at 533.4 eV and a small one at 530.2 eV. The lattice oxygen atoms of the Si–O–Si, Si–O–Ti

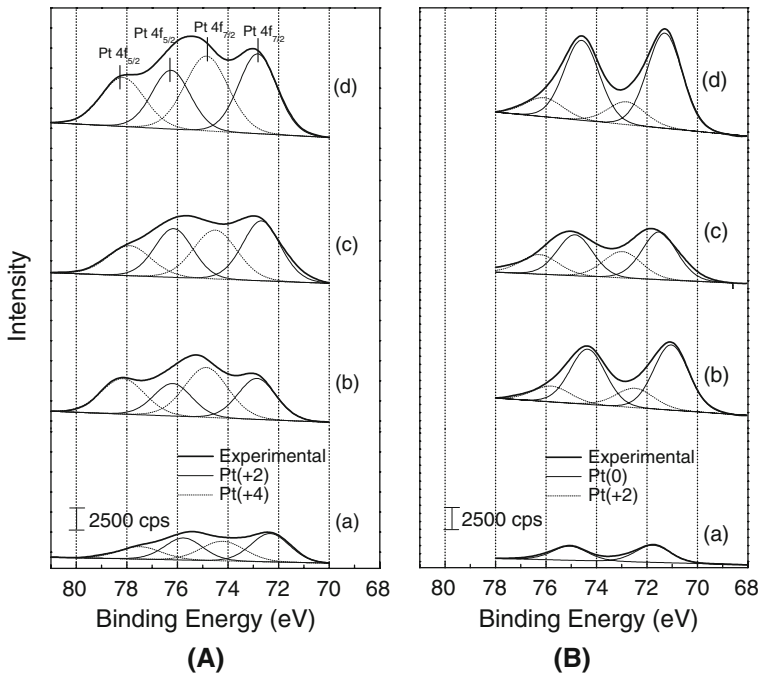


**Fig. 5** XPS spectra of Pt 4f peaks of (a) Pt/SBA, (b) Pt/$H_2O_2$–$TiO_2$–SBA, (c) Pt/$TiO_2$–SBA and (d) $H_2O_2$–Pt/$TiO_2$–SBA catalysts: after drying at **A** 80 °C and reducing at **B** 400 °C

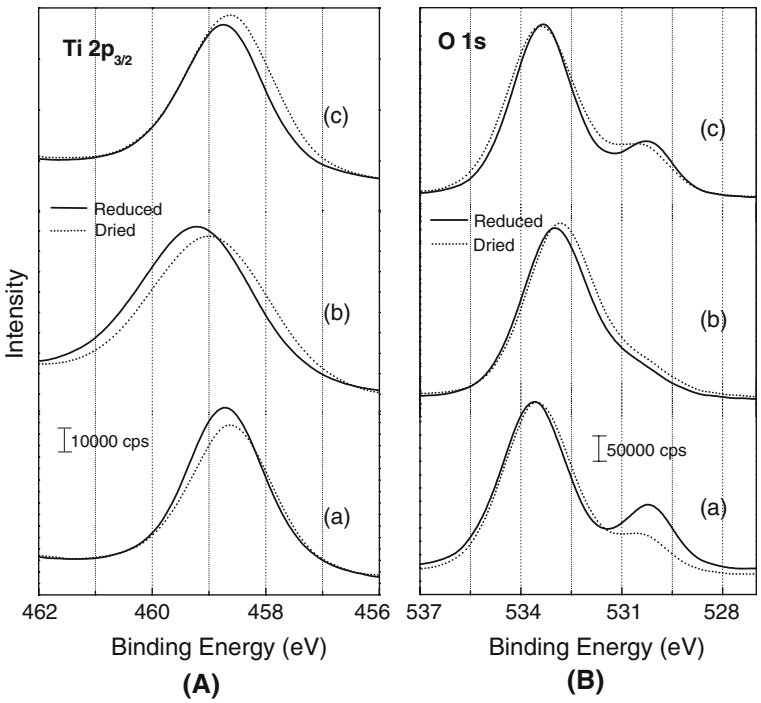


**Fig. 6** XPS spectra of **A** Ti $2p_{3/2}$ and **B** O 1s peaks of (a) Pt/$H_2O_2$–$TiO_2$–SBA, (b) Pt/$TiO_2$–SBA and (c) $H_2O_2$–Pt/$TiO_2$–SBA catalysts

and Ti–O–Ti linkages show their O 1s peak at 534.1, 532.2 and 530.2 eV, respectively [28]. The oxygen atoms of the transition metal oxides, including platinum oxide ($PtO_2$) also show their O 1s peak at 530.2 eV [29, 30].

The small O 1s peak at 530.2 eV appeared on the catalysts supported on the titania-incorporated SBA-15 followed by hydrogen peroxide treatment such as Pt/$H_2O_2$–$TiO_2$–SBA and $H_2O_2$–Pt/$TiO_2$–SBA. The treatment of the titania-incorporated SBA-15 with hydrogen peroxide induced a violent reaction, resulting in the formation of anatase on Pt/$H_2O_2$–$TiO_2$–SBA (Fig. 1). Therefore, the hydrogen peroxide treatment of the platinum precursor can induce the partial oxidation of the platinum precursor to oxidized platinum atoms that have oxygen atoms as the nearest neighbor with a binding energy of 530.2 eV. These results supported the assignment of the small O 1s peak at 530.2 eV on these catalysts to the oxygen atoms in the Ti–O–Ti, Pt–O–Ti and Pt–O–Pt linkages formed on their surface, although no quantitative determination of their fractions was undertaken.

Some of platinum were dispersed on titania and others were chemically bonded on titania through Pt–O–Ti bonds around the outer circle of platinum particles. The hydrogen peroxide treatment caused the coordination of peroxo ($O_2^-$) groups on titanium atoms and increased their electron density. Therefore, the SMSI between platinum and titania caused the increase in the electron density, resulting in the shift of Pt(0) binding energy to lower values, whereas the platinum bonded chemically to titania still retained its oxidation state.

On the other hand, most of oxygen atoms revealed the shift in O 1s peaks were attributed to oxygen atoms of titania, not oxygen atoms in Pt–O–Ti bonds. The hydrogen peroxide treatment caused the coordination of peroxo groups on titanium atoms, increasing the number of oxygen atoms coordinated on them. Therefore, the electron density of each oxygen atom should be decreased.

Raman bands are very sensitive to the presence of crystalline titania [31]. Figure 7 represents Raman spectra of the platinum catalysts supported on the titania-incorporated SBA-15 support. The Pt/$H_2O_2$–$TiO_2$–SBA and $H_2O_2$–Pt/$TiO_2$–SBA catalysts treated with hydrogen peroxide at their preparation showed several Raman bands at 400, 424, 510, 612 and 637 $cm^{-1}$, although the intensities of these bands were very weak. However, the Pt/$TiO_2$–SBA catalyst prepared without the treatment of hydrogen peroxide did not show any definite Raman bands in this range. Since an anatase represents its Raman bands at 400, 510 and 637 $cm^{-1}$ and rutile at 424 and 612 $cm^{-1}$ [31], the observation of these Raman bands clearly show that the treatment with hydrogen peroxide promotes the transformation of incorporated titania layer to crystalline states. A small amount of titania incorporated loosely on SBA-15 became more definite and crystalline state by the treatment with hydrogen peroxide, indicating that the treatment was helpful for titania layer to become more dense states.

The XANES spectra of the platinum catalysts recorded at the dried and reduced states clearly showed the effect of the titania incorporation followed by the hydrogen peroxide treatment on the oxidation state of platinum. Figure 8

displays the XANES spectra of Pt $L_{III}$-edge of the Pt/SBA and $H_2O_2$–Pt/$TiO_2$–SBA catalysts. The XANES spectra of both catalysts before the reduction exhibited only a high peak attributed to oxidized platinum [32]. The absence of any oscillation at higher energy in the XANES spectra confirmed the negligible amount of metallic platinum on these catalysts before the reduction treatment. However, the reduction of the platinum catalysts changed their XANES spectra according to their preparation methods. The signal corresponding to the oxidized platinum of Pt/SBA decreased with the reduction and was accompanied by an increase in the oscillation due to metallic platinum. Although the XANES spectra of $H_2O_2$–Pt/$TiO_2$–SBA also changed similarly to those of Pt/SBA, the extents of the decreased oxidized platinum and the increased oscillation of the metallic platinum were much smaller. This indicated that a relatively large portion of the oxidized platinum of $H_2O_2$–Pt/$TiO_2$–SBA compared to that of Pt/SBA retained its oxidized state even after the reduction treatment.

The EXAFS spectra of the platinum catalysts before and after the reduction treatment, shown in Fig. 9, clearly revealed the variation in the platinum dispersion according to their preparation methods. The chemical state of platinum exhibited no remarkable difference in any of the platinum catalysts after drying at 80 °C. Only the Pt–O atomic pair with R = 1.99 Å was clearly evident on the Fourier transformed radial distributions of platinum, regardless of the preparation method. However, the

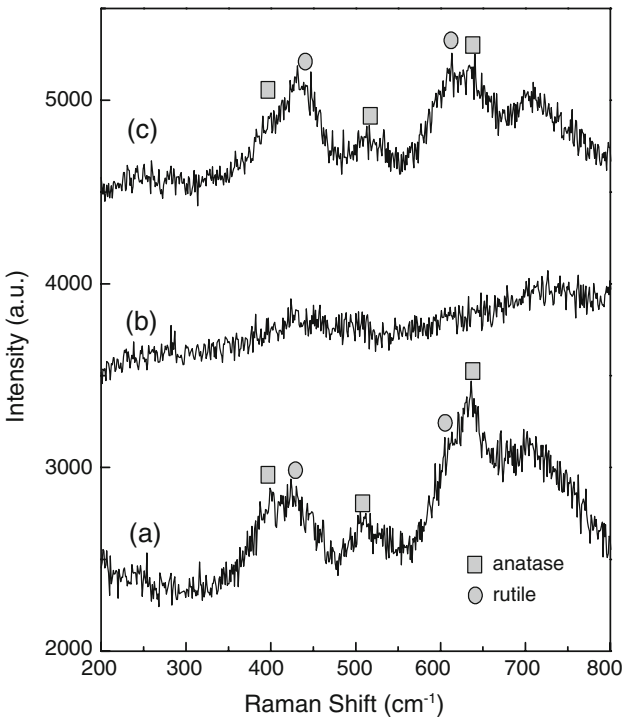


**Fig. 7** Raman spectra of (a) Pt/$H_2O_2$–$TiO_2$–SBA, (b) Pt/$TiO_2$–SBA and (c) $H_2O_2$–Pt/$TiO_2$–SBA catalysts

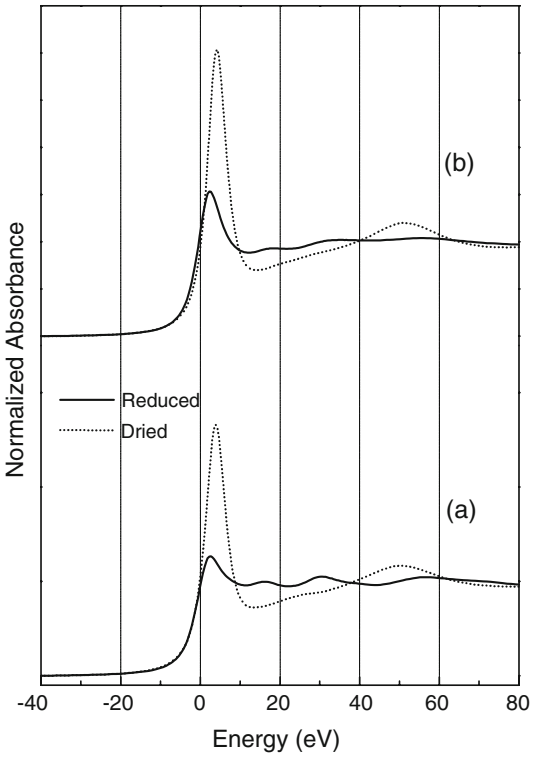


**Fig. 8** Normalized Pt $L_{III}$-edge XANES spectra of (a) Pt/SBA and (b) $H_2O_2$–Pt/$TiO_2$–SBA catalysts

reduction treatment at 400 °C significantly affected the radial distribution of platinum according to the preparation method. Pt/SBA showed a high peak relative to the Pt–Pt atomic pair, indicating the sintering of platinum into large particles. The co-existence of Pt–O and Pt–Pt atomic pairs on Pt/$H_2O_2$–$TiO_2$–SBA indicated that some of the platinum is reduced to metallic state. The large peak attributed to the Pt–Pt atomic pair on it indicated the appreciable *sintering* of platinum atoms. However, the small peaks relative to the Pt–Pt atomic pair at around R = 2.7 Å on Pt/$TiO_2$–SBA and $H_2O_2$–Pt/$TiO_2$–SBA confirmed the high platinum dispersion even after the reduction treatment. The small peak relative to Pt–O at around R = 1.5 Å on $H_2O_2$–Pt/$TiO_2$–SBA indicated that some of the platinum atoms still retained their oxidized state.

EXAFS spectra of the platinum catalysts were recorded in situ in a reductive flow without exposing to air using a specially designed in situ cell [22]. Figure 10 shows Fourier transformed radial distributions of platinum obtained from the EXAFS spectra of the Pt/SBA and $H_2O_2$–Pt/$TiO_2$–SBA catalysts recorded in situ with increasing reduction temperature. The distributions recorded at 25 °C commonly indicated the presence of only Pt–O atomic pairs. However, the reduction at 200 °C induced a large peak relative to Pt–Pt atomic pair on Pt/SBA, indicating the sintering of platinum metals even at low temperature. The increase in the reduction temperature to 400 °C caused the

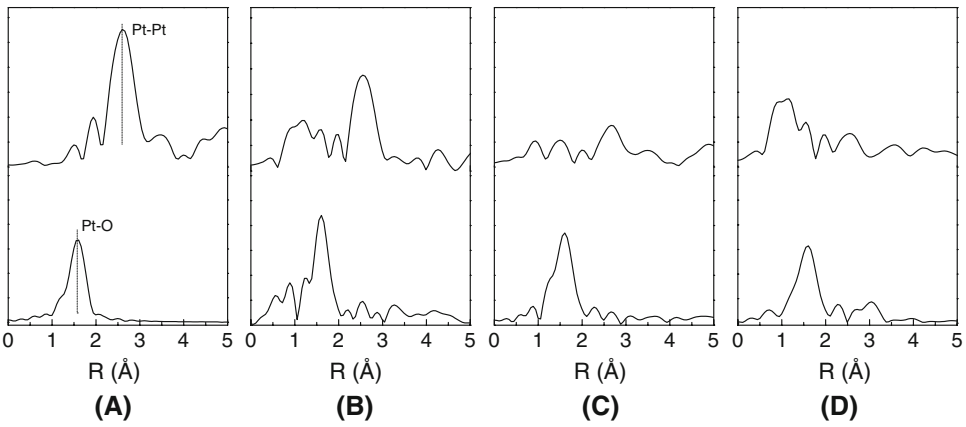


**Fig. 9** Fourier transformed radial distributions of platinum obtained from Pt $L_{III}$-edge EXAFS spectra of **a** Pt/SBA, **b** $Pt/H_2O_2$–$TiO_2$–SBA, **c** $Pt/TiO_2$–SBA and **d** $H_2O_2$–$Pt/TiO_2$–SBA catalysts: lower distributions are recorded after drying at 80 °C and upper ones after reducing at 400 °C

further increase of the peak relative to Pt–Pt atomic pair. No appreciable peak relative to Pt–Pt atomic pair on $H_2O_2$–$Pt/TiO_2$–SBA clearly demonstrated the retention of high dispersion of platinum during the reduction treatment. The high dispersion and stability of platinum on $H_2O_2$–$Pt/TiO_2$–SBA due to the incorporation of titania layer and further treatment with hydrogen peroxide was definitely confirmed from its EXAFS spectra recorded in situ method.

Table 1 lists the amounts of carbon monoxide adsorbed on the platinum catalysts supported on the SBA-15. The adsorption amounts were very small, leading to very low dispersions of platinum if those were calculated from these adsorption amounts. Furthermore, the adsorption amounts of hydrogen on the platinum catalysts also were too small to calculate their platinum dispersion. However, the platinum dispersion on $H_2O_2$–$Pt/TiO_2$–SBA calculated from its TEM images was very high at 87%. These results indicated that the adsorption of carbon monoxide and hydrogen on the platinum particles of the catalysts was strongly suppressed by SMSI or the decoration of titania on the platinum particles at reduced state [15].

The decoration of platinum particles by titania was suggested as a cause for the negligible adsorption of hydrogen on the platinum catalysts supported on titania after reducing at high temperature [18]. If the suppression of hydrogen adsorption on the $H_2O_2$–$Pt/TiO_2$–SBA catalyst was caused by the decoration, the adsorption of benzaldehyde which adsorbed only semiconductors such as tin and titanium oxides could reveal a change in its IR spectra along with the reduction because the exposed surface area of titania should be increased. Figure 11 shows IR spectra of benzaldehyde adsorbed on $TiO_2$–SBA and $H_2O_2$–$Pt/TiO_2$–SBA. Hydroxyl groups formed on the titania layer incorporated on the SBA-15 at the adsorption of benzaldehyde caused a broad band around 3500 $cm^{-1}$. C–H stretching bands of alkyl and aldehyde groups appeared at

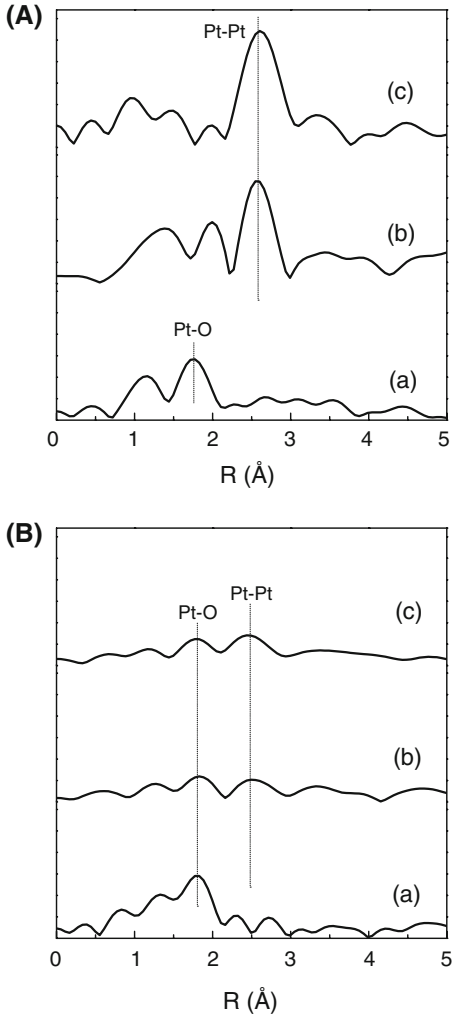


**Fig. 10** Fourier transformed radial distributions of platinum obtained from Pt $L_{III}$-edge EXAFS spectra of **A** Pt/SBA and **B** $H_2O_2$–$Pt/TiO_2$–SBA catalysts. The spectra were recorded in situ in a hydrogen flow with increasing reduction temperature up to (a) 25 °C, (b) 200 °C and (c) 400 °C. The catalysts were evacuated at 200 °C for 2 h prior to exposing to the hydrogen flow

3068, 2857 and 2745 $cm^{-1}$. Carbonyl groups of benzaldehyde adsorbed caused a large band at 1695 $cm^{-1}$ [19]. Benzaldehyde adsorbed on the reduced $TiO_2$–SBA induced a higher IR spectrum compared to its calcined state, while that adsorbed on the reduced $H_2O_2$–Pt/$TiO_2$–SBA induced a lower IR spectrum. The removal of excess oxygen on $TiO_2$–SBA during the reduction treatment led the exposure of more titania, resulting in the increase of absorption bands relative to benzaldehyde. If the decoration of platinum particles with titania occurred at the reduction treatment of $H_2O_2$–Pt/$TiO_2$–SBA, the IR spectrum of benzaldehyde adsorbed on it after the reduction should be equal or higher compared to that adsorbed the calcined state. The small adsorption of benzaldehyde on the reduced $H_2O_2$–Pt/$TiO_2$–SBA indicated that the decoration was not certain on the platinum catalyst supported on the titania-incorporated SBA-15.

Unusual adsorption of hydrogen and carbon monoxide on platinum catalysts dispersed on titania support after reduction at high temperature is usually explained by the decoration of platinum with titania [23–25]. Titania migrates to the exposed surface of platinum particles and reduces effective platinum atoms for their adsorption. However, the migration and expansion of titania on the platinum atoms of $H_2O_2$–Pt/$TiO_2$–SBA after the reduction treatment were not observed in the adsorption of benzaldehyde. The decoration of platinum, thus, was not only a plausive explanation for the suppression of hydrogen adsorption on the platinum catalysts supported on the titania layer-incorporated SBA-15. The change in the electronic state of platinum due to the strong interaction with titania also causes a large reduction of hydrogen adsorption.

In situ EXAFS and XPS spectra strongly suggested the presence of oxidized platinum atoms as well as metallic platinum atoms even after the reduction. This suggested that the oxidized platinum atoms had oxygen atoms as the nearest neighbor and combined with titanium atoms through Pt–O–Ti bands at the interface between platinum particles and titania layer. The formation of Pt–O–M (M:Ce, Mg, Zr, Ti) bonds on platinum catalysts supported on various supports were reported based on their EXAFS spectra [3, 33]. These bonds were responsible for both the high dispersion and stability of platinum. The strong interaction between platinum and titania enhances the stability of platinum even at the reduction treatment, the Pt–O–Ti bands encircled platinum particles suggested on $H_2O_2$–Pt/$TiO_2$–SBA also suppress the sintering of platinum.

The catalytic activity of the platinum catalysts in the combustion reactions of carbon monoxide and methane strongly depended on their preparation methods, as shown in Fig. 12. Despite the same 4 wt.% platinum loading, the light-off temperature for the combustion of carbon monoxide varied considerably. $H_2O_2$–Pt/$TiO_2$–SBA showed the lowest light-off temperature of 188 °C, while that of Pt/SBA was too high to be measured in the experimental temperature range. A similar trend was also observed in the combustion of methane. $H_2O_2$–Pt/$TiO_2$–SBA with the highest platinum dispersion also showed the lowest light-off temperature.

Although the platinum catalysts in the catalytic combustion of carbon monoxide and methane exhibited the same order, their catalytic activities in these two combustion reactions showed notable differences. The Pt/$TiO_2$–SBA, Pt/$H_2O_2$–$TiO_2$–SBA and $H_2O_2$–Pt/$TiO_2$–SBA catalysts supported on the titania-incorporated SBA-15 showed relatively high activity in the combustion of carbon monoxide, regardless of the hydrogen peroxide treatment. The high activity was due to the activation of carbon monoxide on the titania [18], and thus the difference in the platinum

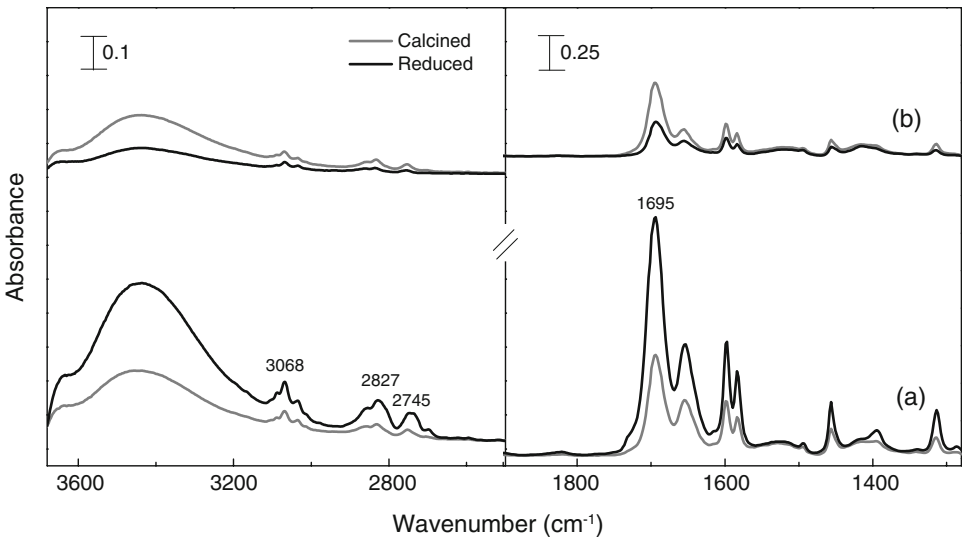


**Fig. 11** FT-IR spectra of benzaldehyde adsorbed on (a) $TiO_2$–SBA and (b) $H_2O_2$–Pt/$TiO_2$–SBA. The IR spectra were recorded after calcinations at 400 °C and reduction with hydrogen at 400 °C, respectively

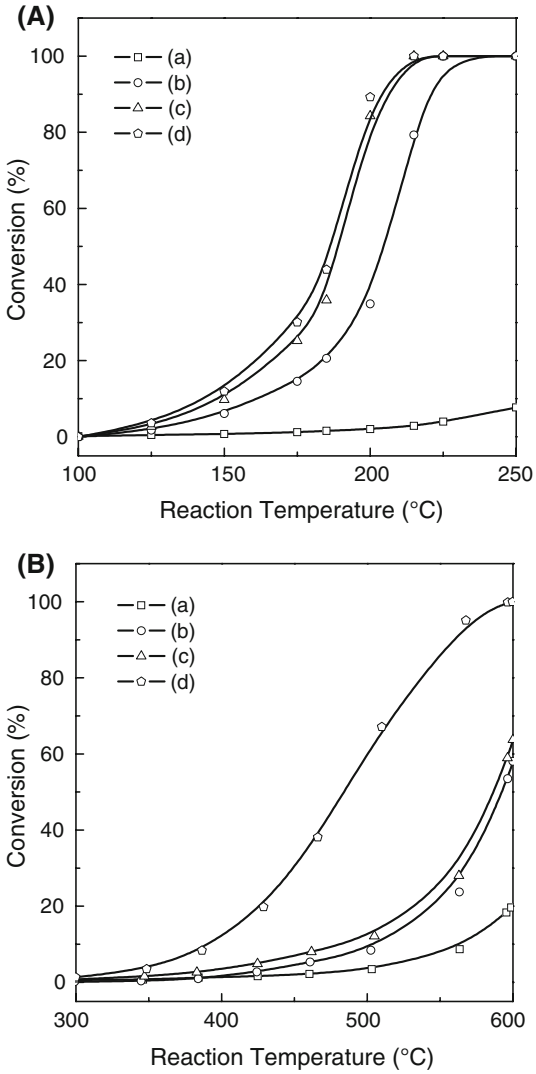


**Fig. 12** Catalytic performance of (a) Pt/SBA, (b) $Pt/H_2O_2–TiO_2–SBA$, (c) $Pt/TiO_2–SBA$ and (d) $H_2O_2–Pt/TiO_2–SBA$ catalysts in **A** the oxidation of carbon monoxide and **B** the combustion of methane

dispersion did not greatly influence the activity of these catalysts in the combustion of carbon monoxide. On the contrary, $Pt/TiO_2–SBA$ and $Pt/H_2O_2–TiO_2–SBA$ exhibited notably lower activity in the combustion of methane. Since the activation of both methane and oxygen on platinum was required in the combustion of methane [34], the platinum catalyst with the greatest dispersion, $H_2O_2–Pt/TiO_2–SBA$, showed the highest activity in the combustion reactions. It is very reasonable that the catalytic activity of the platinum catalysts in the combustion of methane was strongly dependent on the platinum dispersion. Even the platinum catalysts supported on the titania-incorporated SBA-15 exhibited poor catalytic activities when the platinum dispersion on them was not sufficiently high.

The wide application of diesel vehicles strongly requires the removal of carbon monoxide, unburned hydrocarbons and solid organic fractions from their emission. Diesel oxidation catalysts prepared by impregnating platinum on alumina are installed in heavy trucks and urban buses. Since the catalysts are working at a wide temperature range for a long time, the dispersed platinum needs to retain its active state after long-term operation. The other requirement for diesel oxidation catalysts is high activity at low temperature because the exhaust gas temperature is reduced in highly advanced diesel engines to enhance their fuel efficiency and to reduce their $NO_x$ emissions [35]. Tin has been added to the platinum catalyst for diesel soot oxidation [36]. A screening study on suitable supports for diesel oxidation catalysts has also been reported [37]. The supports containing ceria showed better stability in the presence of water. However, platinum catalysts supported on titania-incorporated SBA-15 and treated with hydrogen peroxide were confirmed in the present study to be very suitable for application as diesel oxidation catalysts due to their high activity in the combustion reactions of both carbon monoxide and methane. Furthermore, their high stability at higher temperatures holds the promise of high performance for long-term, realistic application. A practical application test of the platinum catalysts for the oxidative removal of hydrocarbon and carbon monoxide from diesel engine exhausts is now being conducted. The details will be presented in a future paper.

## 4 Conclusions

The hydrogen peroxide treatment of a hydrogen hexahydroxyplatinate precursor impregnated on titania-incorporated SBA-15, followed by calcination and reduction, produced an exceptionally well dispersed and stable platinum catalyst. The uniformly dispersed platinum particles ranged 1–2 nm in size and were stable at 850 °C in a reductive atmosphere, even at a platinum loading as high as 4 wt.%. Titania incorporated onto the SBA-15 exhibited a tetrahedral coordination and stabilized platinum particles. The hydrogen peroxide treatment of the platinum precursor impregnated on the titania-incorporated SBA stabilized titania layer and suggested to promote the formation of Pt–O–Ti linkages. Therefore, the high stability and dispersion of platinum on $H_2O_2–Pt/TiO_2–SBA$ were resulted from the stabilization of platinum by the strong interaction with titania and the suppressing of platinum *sintering* by these linkages. The high activity and stability of the platinum catalyst in combustion reactions of both carbon monoxide and methane confirmed its suitability as a diesel oxidation catalyst.

**Acknowledgements** This work is a part of the project "Development of Partial Zero Emission Technology for Future Vehicles"

funded by the Ministry of Knowledge Economy and we are grateful for its financial support. We acknowledge the Pohang Accelerator Laboratory (PAL) for the XAS measurement.

## References

1. Rase HF (2000) Handbook of commercial catalysts-heterogeneous catalysts. CRC Press, Boca Raton, p 105
2. Yu X, Ye S (2007) J Power Sources 172:133
3. Nagai Y, Hirabayashi T, Dohmae K, Takagi N, Minami T, Shinjoh H, Matsumoto S (2006) J Catal 242:103
4. Kuriyama M, Tanaka H, Ito S, Kubota T, Miyao T, Naito S, Tomishige K, Kunimori K (2007) J Catal 252:39
5. Wu G, Chen T, Zong X, Yan H, Ma G, Wang X, Xu Q, Wang D, Lei Z, Li C (2008) J Catal 253:225
6. Silvestre-Albero J, Coloma F, Sepúlveda-Escribano A, Rodríguez-Reinoso F (2006) Appl Catal A 304:159
7. Ma H, Wang L, Chen L, Dong C, Yu W, Huang T, Qian Y (2007) Catal Commun 8:452
8. Mukherjee S, Vannice MA (2006) J Catal 243:108
9. Douidah A, Marécot P, Barbier J (2002) Appl Catal A 225:11
10. Meephoka C, Chaisuk C, Samparnpiboon P, Praserthdam P (2008) Catal Commun 9:546
11. Hu L, Boateng KA, Hill JM (2006) J Mol Catal A 259:51
12. Oudenhuijzen MK, Kooyman PJ, Tappel B, Bokhoven JA, Koningsberger DC (2002) J Catal 205:135
13. Goguet A, Schweich D, Candy JP (2003) J Catal 220:280
14. Kim MY, You YS, Han HS, Seo G (2008) Catal Lett 120:40
15. Silvestre-Albero J, Sepúlveda-Escribano A, Rodríguez-Reinoso F, Anderson JA (2004) J Catal 223:179
16. Sayari A, Yang Y (2005) Chem Mater 17:6108
17. Du J, Kuang W, Xu H, Shen W, Zhao D (2008) Appl Catal B 84:490
18. Foger K (1984) In: Anderson JR, Boudart M (eds) Catalysis science and technology, vol 6, Chap 4. Springer-Verlag, Berlin, p 237
19. Niwa M, Suzuki K, Kishida M, Murakami Y (1991) Appl Catal 67:297
20. Ravikumar C, Joe IH, Jayakumar VS (2008) Chem Phys Lett 460:552
21. Zhao D, Huo Q, Feng J, Chmelka BF, Stucky GD (1998) J Am Chem Soc 120:6024
22. Lee WJ, Jung HR, Kim MY, Cho SJ, Seo G, Jang YB Korea Patent 10-2007-0023232
23. Weerachawanasak P, Praserthdam P, Arai M, Panpranot J (2008) J Mol Catal A 279:133
24. Azzan KG, Babich IV, Seshan K, Lefferts L (2008) Appl Catal A 338:66
25. Ruppert AM, Paryjczak T (2007) Appl Catal A 320:80
26. Zhang W, Li Y, Zhu S, Wang F (2004) Surf Coat Technol 182:192
27. Schwartz V, Mullins DR, Yan W, Zhu H, Dai S, Overbury SH (2007) J Phys Chem C 111:17322
28. Almeida RM, Vasconcelos HC, Goncalves MC, Santos LF (1998) J Non-Cryst Solids 232:65
29. Mei F, Liu C, Zhang L, Ren F, Zhou L, Zhao WK, Fang YL (2006) J Cryst Growth 292:87
30. Silva LA, Alves VA, Castro SC, Boodts JFC (2000) Colloid Surf A 170:119
31. Evans P, English T, Hammond D, Pemble ME, Sheel DW (2007) Appl Catal A 321:140
32. Shishido T, Tanaka T, Hattori H (1997) J Catal 172:24
33. Tanabe T, Nagi Y, Dohmae K, Sobukawa H, Shinjoh H (2008) J Catal 257:117
34. Wei J, Iglesia E (2004) J Phys Chem B 108:4094
35. Komatsu T, Tomokuni K, Yamada I (2006) Catal Today 116:244
36. Corro G, Fierro JLG, Romero FB (2006) Catal Commun 7:867
37. Becker E, Thormählen P, Maunula T, Suopanki A, Skoglundh M (2007) Top Catal 42–43:421